THE ASTROPHYSICAL JOURNAL, 329:618–628, 1988 June 15

BURSTING DWARF GALAXIES: IMPLICATIONS FOR LUMINOSITY FUNCTION, SPACE DENSITY, AND COSMOLOGICAL MASS DENSITY

NEIL D. TYSON AND JOHN M. SCALO
University of Texas, Department of Astronomy
Received 1986 August 7; accepted 1987 December 7

ABSTRACT

The possibility that dwarf irregular and blue compact galaxies undergo episodes of star formation bursts leads to the suspicion that a large fraction of these galaxies remain undetected because of observational selection effects involving limiting magnitude, surface brightness, and angular size. We have attempted to estimate this unobserved fraction by comparing simulated samples of bursting galaxies, constructed using the theoretical results of Gerola, Seiden, and Schulman, with a magnitude-limited catalog of real dwarf and blue compact galaxies. Assuming a frequency distribution of galaxy sizes of the form $f(r) = r^{\gamma}$, we find that, after correcting the simulated catalog for selection effects, a value of $\gamma = -4.2 \pm 0.2$ gives good agreement with the observed frequency distributions of luminosity, optical radius, and angular size. The same model accounts for the observed luminosity function in the Virgo cluster. The implications of this result for the true shape of the galaxy luminosity function and the contribution to the cosmological density are discussed.

Subject headings: galaxies: evolution — galaxies: photometry — galaxies: stellar content — luminosity function — stars: formation

I. INTRODUCTION

The detection of galaxies is limited by apparent magnitude, surface brightness, and angular size (e.g., Arp 1965; Disney 1976). For these reasons it is possible that a large number of galaxies remain unidentified. That these unseen galaxies may be composed largely of dwarf irregular galaxies is suggested by two considerations: (1) The local group consists mostly of dwarf galaxies. Of these, the dwarf irregulars (e.g., IC 1613 and NGC 6822) are so faint, small, and/or have such a low surface brightness that they would be invisible at much larger distances. (2) It is currently believed that small gas-rich dwarf galaxies undergo irregular or intermittent episodes of star formation on the basis of their colors, hydrogen line strengths, and other properties. (For a review see Hunter and Gallagher 1986.) The blue compact and H II galaxies are the most extreme examples. The models for stochastic self-propagating star formation (SSPSF) in dwarf galaxies by Gerola, Seiden, and Schulman (1980) predict bursting behavior, with the burst amplitude and duty cycle increasing with decreasing galaxy size. These considerations lead to the suspicion that most dwarf galaxies, especially the smaller ones, may be in an unobservable nonbursting state.

We have attempted to estimate the true average space density of gas-rich dwarf galaxies by comparing the luminosity and size distributions of visible dwarf irregulars with a set of simulated observations of a bursting population of galaxies on which selection effects corresponding to the real observations have been imposed. The true size distribution is assumed to be a power law, $f(r) \propto r^{\gamma}$, and the exponent γ is the free parameter whose value we wish to estimate.

II. THE OBSERVED SAMPLE

The real sample was obtained by combining the radio (H I) surveys of DDO dwarfs (van den Bergh 1959) by Fisher and Tully (1975) and of Nilson dwarfs (Nilson 1973) by Thuan and Seitzer (1979). The DDO catalog and the Nilson dwarfs contain a mixture of dwarf irregulars, dwarf spheroidals, and dwarf ellipticals. The spheroidals and ellipticals are devoid of gas and are not expected to undergo star formation in the current epoch. They were omitted from the assembled data set.

The photoelectric aperture photometry of DDO dwarfs by de Vaucouleurs, de Vaucouleurs, and Buta (1981, 1983), Longo and de Vaucouleurs (1983, 1985), and Buta (1986) was used for magnitudes and colors. The diameters and masses, based on H I velocity widths, were taken from Fisher and Tully (1975) and Thuan and Seitzer (1979).

There were 74 galaxies brighter than B_T^0, which is where the apparent magnitude distribution turns over (see Fig. 1). These 74 galaxies fell within the following limits: $1.0 \leq r_{26.5} \leq 12.3$ kpc (where $r_{26.5}$ is the radius at the 26.5 mag arcsec^{-2} isophotal surface birghtness), angular diameter $2'.6 \leq \theta \leq 28'$, mean surface brightness $23.0 \leq m'_{26.5} \leq 26.3$ mag arcsec^{-2} (where $m'_{26.5}$ is the mean surface brightness within 26.5 mag arcsec^{-2} isophote), and $-12.5 \leq M_B \leq -18.0$ ($H_0 = 100$ km s^{-1} Mpc^{-1}).

The frequency distributions of these quantities are shown in Figures 2*a*–2*c*. Notice that they turn over well before their dimmest/smallest limit. Since all selection effects are not entirely independent of each other, they simultaneously play a role in detection. The completeness limit for any single observable therefore cannot be defined by its turnover when the sample is preselected by apparent magnitude (cf. de Vaucouleurs 1975).

The 74 dwarf galaxies are listed in Table 1 and were used as a data set with well-defined selection limits for comparison with the theoretical simulations.

The key to the columns for Table 1 is as follows:

Column (1).—Identification number. Galaxies that begin with "D" represent the catalog number in the David Dunlop Observatory (DDO) catalog of dwarf galaxies (van den Bergh 1959). Galaxies that begin with "U" represent the catalog number in the Uppsala General Catalog (UGC) of galaxies (Nilson 1973).

TABLE 1

MAGNITUDE-LIMITED CATALOG OF DWARF IRREGULAR GALAXIES

(1) ID	(2) α	(3) δ	(4) B_T^o	(5) θ	(6) M_B	(7) $m'_{26.5}$	(8) Δ	(9) $r_{26.5}$	(10) $M/10^9$
U0099	0h 8.m1	13°25'	13.4	4.3	-18.0	24.8	19.27	12.05	1.7
D223	0 11.5	-23 27	11.0	9.4	-17.5	24.0	5.04	6.8	17.0
D156	0 14.2	12 4	12.9	4.3	-17.7	24.2	13.10	8.19	2.2
D2	0 17.5	10 36	13.6	3.8	-17.0	24.7	12.90	7.13	12.0
D8	1 2.3	1 52	9.8	27.7	-14.2	25.2	0.64a	2.58	0.12
D14	1 46.0	-12 37	13.5	4.3	-17.6	24.8	16.34	10.22	8.0
D19	2 22.0	35 48	13.6	4.9	-15.7	25.2	7.12	5.07	2.8
D25	2 30.3	33 16	13.5	4.3	-15.8	24.8	7.41	4.63	1.4
D24	2 30.5	40 18	13.7	4.9	-15.6	25.3	7.23	5.15	2.1
D28	2 45.4	3 40	13.1	7.5	-17.0	25.7	10.60	11.56	10.0
D29	2 46.6	1 55	13.8	7.5	-16.5	26.3	11.31	12.34	11.0
D32	3 12.2	-4 57	13.8	2.9	-17.9	24.3	22.00	9.28	14.0
D228	4 47.2	-29 17	12.8	4.5	-17.8	24.2	13.20	8.64	3.8
D230	5 8.8	-31 40	12.7	3.8	-16.8	23.8	8.12	4.4	2.5
D231	5 10.1	-33 1	13.0	4.8	-16.4	24.6	7.63	5.33	2.3
D232	5 17.9	-32 12	12.8	3.1	-17.4	23.4	10.73	4.84	2.1
U3303	5 22.3	4 27	12.1	5.4	-16.1	23.9	4.30	3.38	7.6
D39	5 49.9	75 18	13.6	6.5	-16.3	25.8	9.71	9.18	1.4
U3475	6 27.0	39 32	12.6	4.1	-15.9	23.9	5.09	3.04	4.3
D42	7 23.6	69 18	10.8	10.0	-16.4	24.0	2.75f	3.99	1.8
D47	7 39.1	16 55	13.1	6.5	-13.6	25.3	2.19	2.07	0.08
D49	8 7.6	46 36	13.9	2.9	-17.9	24.4	22.78	9.61	7.5
D50	8 13.9	70 52	10.8	11.0	-16.4	24.8	2.75b	4.41	1.3
D63	9 36.0	71 24	12.7	5.3	-14.8	24.5	3.16f	2.44	0.15
D235	9 42.6	-31 36	12.8	3.3	-17.2	23.6	0.17	4.88	6.3
D69	9 56.5	30 59	12.5	7.0	-12.5	24.9	1.00e	1.02	0.09
D70	9 57.4	5 33	11.6	7.7	-13.4	24.2	1.00e	1.12	0.14
D236	10 0.8	-25 55	10.2	17.2	-14.8	24.6	1.00e	2.50	0.92
D75	10 8.5	-4 26	11.3	9.3	-15.0	24.3	1.78b	2.41	0.75
D77	10 20.2	71 7	12.5	4.9	-17.8	24.1	11.35	8.09	11.0
D81	10 24.8	68 40	10.7	16.0	-16.7	24.9	3.05c	7.09	2.6
D238	10 33.0	-24 29	12.9	4.8	-16.7	24.5	8.28	5.78	3.0
D84	10 39.8	34 42	13.5	4.3	-15.4	24.9	6.12	3.83	2.8
D94	11 17.7	2 47	13.5	3.7	-17.4	24.5	14.76	7.94	4.3
D95	11 21.8	3 35	12.9	3.0	-17.6	23.5	12.50	5.45	4.8
D99	11 48.2	39 9	13.3	11.3	-13.8	26.7g	2.65c	4.35	0.28
D105	11 55.9	38 20	13.6	7.5	-16.3	24.2	9.34	10.19	9.7
D119	12 18.2	46 34	13.1	4.3	-15.8	24.5	5.90	3.69	6.2
D120	12 18.8	46 5	13.2	4.0	-15.4	24.4	5.19	3.02	0.28
D122	12 22.1	70 36	12.8	5.4	-16.1	24.6	6.08	4.78	0.8
D123	12 23.8	58 35	12.6	4.9	-17.0	24.2	8.25	5.88	2.0
U7557	12 24.7	7 32	13.6	4.5	-16.0	25.1	8.26	5.44	14.0
D125	12 25.3	43 46	12.7	5.9	-15.8	24.7	4.90c	4.20	0.24
D129	12 26.3	43 30	13.5	5.4	-15.4	25.3	5.91	4.64	1.2
D133	12 30.4	31 48	13.0	8.6	-14.7	25.9	3.42	4.28	1.2
D138	12 34.1	6 53	13.1	4.3	-17.2	24.5	12.00d	7.53	1.4
D141	12 39.8	38 46	13.6	5.4	-14.9	25.5	4.90c	3.86	0.57
D142	12 41.5	-5 24	12.7	4.6	-17.9	24.2	13.11	8.77	9.1
D144	12 41.9	0 46	12.6	4.2	-17.6	23.9	10.85	6.63	6.3
D146	12 43.1	-5 48	13.7	4.6	-17.0	25.2	13.60	9.10	2.8
D150	12 46.1	51 26	13.2	3.7	-15.5	24.2	5.52	2.97	0.58
D154	12 51.7	27 25	13.8	3.7	-14.1	24.8	3.79	2.04	1.3
D161	13 0.7	-17 9	13.3	6.0	-15.6	25.4	6.05	5.28	2.3
U8188	13 3.5	37 52	11.4	7.1	-16.9	23.9	4.48	4.65	0.46
D166	13 11.0	34 28	13.3	3.2	-16.7	24.0	9.99	4.65	1.8
D168	13 12.2	46 10	12.5	9.3	-14.7	25.5	2.75c	3.71	5.9
D175	13 23.5	58 4	13.6	4.9	-17.5	25.2	16.37	11.67	11.0
D179	13 34.9	7 53	13.0	5.4	-17.0	24.8	10.11	7.94	8.5
D180	13 35.5	-9 33	12.5	3.2	-17.9	23.2	12.03	5.60	3.3
D242	13 38.8	-29 39	13.7	3.0	-14.3	24.2	3.85	1.68	0.4
D185	13 52.9	54 8	13.6	6.5	-14.9	25.8	5.01b	4.74	0.96
D184	13 53.0	18 2	13.8	4.6	-16.1	25.3	9.70	6.49	5.3
D190	14 22.8	44 45	13.1	3.1	-15.2	23.8	4.48c	2.03	0.43
D196	14 42.9	8 4	13.5	4.3	-17.6	24.9	16.97	10.61	3.3
D203	14 47.9	81 57	13.3	4.5	-17.8	24.8	16.87	11.04	16.0
D204	16 14.8	47 10	13.3	4.5	-16.4	24.7	8.83	5.78	3.5
D209	19 42.1	-14 55	8.3	20.0	-15.4	23.0	0.56a	1.63	0.48
U11891	22 1.5	43 30	12.1	5.4	-17.3	23.9	7.53	5.89	9.1
D213	22 31.9	32 35	13.7	4.9	-16.4	25.3	10.38	7.40	8.3
D216	23 26.0	14 28	11.9	7.7	-13.1	24.5	1.00	1.12	0.10
D217	23 27.5	40 43	12.2	6.5	-16.9	24.4	6.49	6.14	7.9
D218	23 32.3	17 57	13.8	2.6	-17.2	24.0	15.80	5.97	2.3
U12732	23 38.2	25 57	13.2	4.3	-16.8	24.6	9.85	6.19	3.9
D221	23 59.4	-15 44	11.1	12.6	-15.3	24.5	1.63b	2.98	0.5

Columns (2), (3).—Right ascension, α, in hours and minutes. Declination, δ, in degrees and arc minutes for the 1950.0 equinox.

Column (4).—Total apparent *B* magnitude corrected for galactic and Galactic extinction taken from de Vaucouleurs, de Vaucouleurs, and Buta (1983) and Buta (1986).

Column (5).—Angular diameter at the 26.5 mag arcsec^{-2} isophote measured in arc minutes.

Column (6).—Absolute magnitude in the *B* band computed from columns (4) and (8).

Column (7).—Mean surface brightness in mag arcsec^{-2} within $r_{26.5}$.

Column (8).—Distances for most of these objects are computed using $H_0 = 100$ km s^{-1} Mpc^{-1} where the galaxy's redshift was corrected for solar motion as given in Fisher and Tully (1975) and Thuan and Seitzer (1979). The remainder are footnoted.

Column (9).—The galaxy radius at the $\mu = 26.5$ mag arcsec^{-2} isophote computed from columns (5) and (8).

Column (10).—Total "indicated" mass in 10^9 solar units taken from Fisher and Tully (1975) and Thuan and Seitzer (1979). It has the form

$$M_T = (5 \times 10^3) D\, 2r_{26.5}(\Delta v)^2 ,$$

where *D* is the distance in Mpc, $r_{26.5}$ is the radius at the 26.5 mag arcsec^{-2} isophote measured in arc minutes (the Holmberg 1958 radius), and Δv is the H I velocity width in kilometers per second at 50% peak intensity. The following 30 galaxies have their total mass approximated (based on the statistics of the rest of the data set) from $M_T = 4 \times (1.34 M_{\rm H\,I})$ when the indicated mass was not available (details are in § VI): DDO 8, 25, 24, 28, 29, 228, 230, 232, 49, 63, 235, 69, 75, 238, 84, 95, 122, 129, 138, 146, 150, 154, 166, 175, 180, 242, 190, 196, 209, and 213. The masses for UGC 0099, 8188, and 12732 are uncorrected for inclination since they are nearly face-on. The values quoted should be considered lower limits.

III. THE SIMULATED SAMPLE

The simulations are based on the bursting dwarf galaxy models of Gerola, Seiden, and Schulman (1980, hereafter GSS) and (Seiden 1983, 1986). The average values of peak burst luminosity, time scale for luminosity decline after the burst peak, quiescent luminosity, and time between bursts as a function of galaxy radius were estimated from graphs presented by GSS.

In an effort to preserve and model as much of the information given by GSS as possible, we repesented the form of the luminosity decline for each burst as an exponential. We assumed an exponential frequency distribution for the time between bursts where the mean was taken to be a function of the galaxy radius. We also distributed the luminosity of

[a] Distances to DDO 8 and 209 are taken from de Vaucouleurs 1978*a*.

[b] Distances to DDO 50, 75, 185, and 221 are taken from de Vaucouleurs 1978*b*.

[c] Distances to DDO 81, 99, 125, 141, 168, and 190 are taken from de Vaucouleurs 1975 and de Vaucouleurs 1979.

[d] Distance to DDO 138 is assigned Virgo cluster membership at $D = 16$ Mpc.

[e] DDO 69, 70, and 236 are Local Group galaxy members that are arbitrarily assigned $D = 1$ Mpc.

[f] Distances to DDO 42 and 63 are taken from de Vaucouleurs, de Vaucouleurs and Buta 1983.

[g] Due to size and distance uncertainties, DDO 99 has $m'_{26.5} = 26.7$ mag arcsec^{-2}.

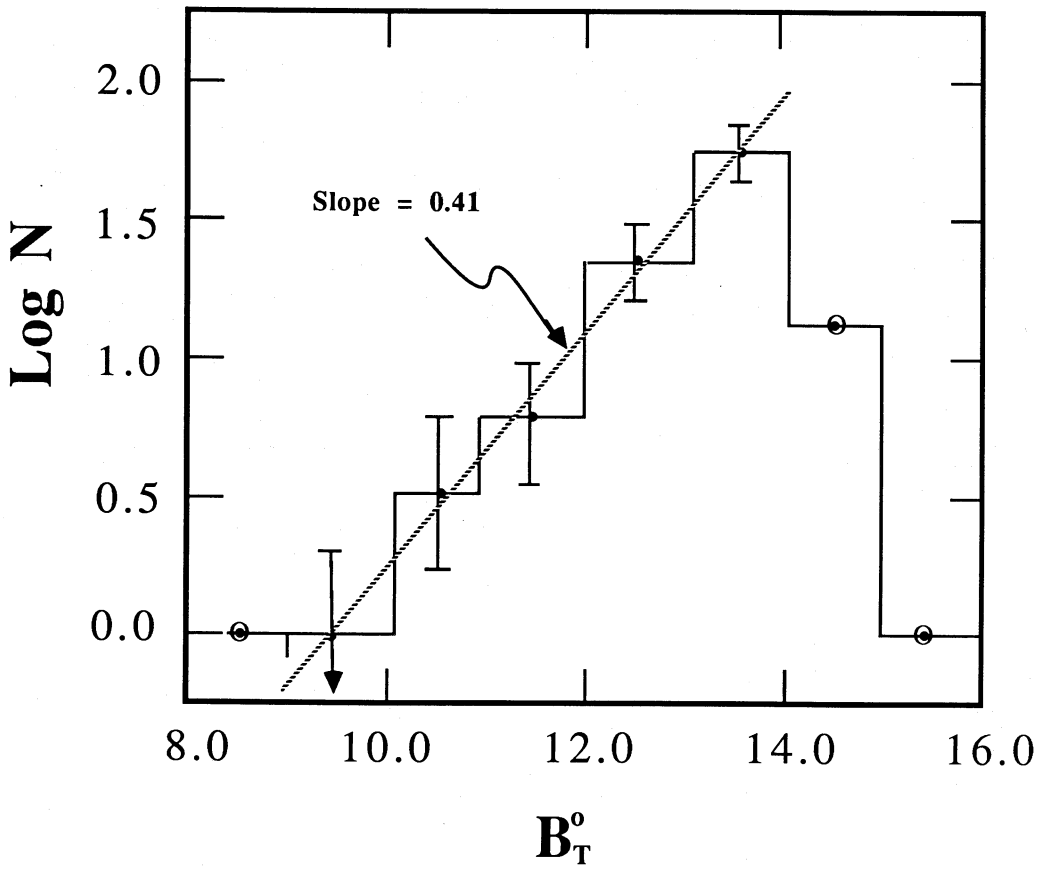

FIG. 1.—The B magnitude distribution of dwarf irregular galaxies from the DDO (van den Bergh 1959) and Nilson (1973) catalogs. There are 74 galaxies brighter than $B_T^0 = 14$. The line is a least-squares fit where the circled points are not included.

the peaks for each burst according to the relation $f(L_{\rm peak}) \propto L_{\rm max}(1 - s^n)$, where s is a random number uniformly distributed on (0, 1), $n = 3$, and $L_{\rm max}$ is the largest peak luminosity expected from the galaxy. A large n will favor large bursts, while $n = 0$ will generate small bursts as frequently as large bursts. These distributions are somewhat uncertain but are consistent with the information given in GSS, and it will be seen later that our results turn out to be reasonably insensitive to the adopted distributions.

The area (and corresponding radius) of a simulated galaxy was defined as the region within which the neutral hydrogen column density was above a threshold for detectable (OB) star formation to occur. Gallagher and Hunter (1984) suggest a threshold density of $N_{\rm H\,I} = 5 \times 10^{20}$ cm^{-2}. We expect this threshold to coincide roughly with the Holmberg (1958) radius (the radius of a galaxy at its 26.5 mag arcsec^{-2} isophote) based on the data given in Huchtmeier *et al.* (1981), Skillman *et al.* (1985), and Skillman and Bothun (1986).

The Holmberg radius, $r_{26.5}$, is not as easily measured as other radii such as r_e (the effective radius within which half the total light is emitted), or r_{25}. The fact that some low surface brightness galaxies do not have an r_{25} anywhere across their surface (e.g., Buta 1986, 1987; Bothun, Impey, and Malin 1986), and that the 26.5 mag arcsec^{-2} isophote has been identified with a critical gas density for star formation, makes $r_{26.5}$ a very useful quantity for modeling purposes.

The estimated size of a galaxy at any given isophote can be determined immediately from its luminosity profile. Larger dwarfs and many blue compact dwarf galaxies (BCDs) have been observed to have exponential disks (e.g., Bothun *et al.* 1986; Kunth *et al.* 1985; Loose and Thuan 1985), but there is over a factor of 2 range in scale lengths. Smaller dwarfs show very little central concentration of light (if any concentration at all) and are best described with an exponential disk only in the "equivalent radius" (e.g., de Vaucouleurs and Freeman 1972) which is an abstract quantity that maps knotty, irregular morphologies into a circularly symmetric, centrally condensed luminosity profile.

In this study we are not concerned with the morphological details of a galaxy's surface. For simplicity, all simulated galaxies were given a flat luminosity profile. Their mean effective surface brightness, therefore, equaled the mean surface brightness of their entire star forming region. To treat the real dwarf galaxies as though they had flat profiles requires the computation of $m'_{26.5}$ by taking the ratio: $m'_{26.5} \propto B_T^0/(r_{26.5})^2$. This is a valid approximation as long as a significant fraction of the flux that contributes to B_T^0 is *not* emitted outside the 26.5 mag arcsec^{-2} isophote. For example, a galaxy with as much as 20% of its light emitted outside the 26.5 mag arcsec^{-2} isophote will have an $m'_{26.5}$ that is 0.2 mag too bright. No known profile is this extreme, and none are expected to be, especially when we consider the 26.5 mag arcsec^{-2} isophote to correspond with a star formation threshold.

The frequency distribution of sizes was assumed to be a power law, $f(r) \propto r^\gamma$, with exponent γ to be determined. An ensemble of over 10^5 simulated galaxies was constructed and

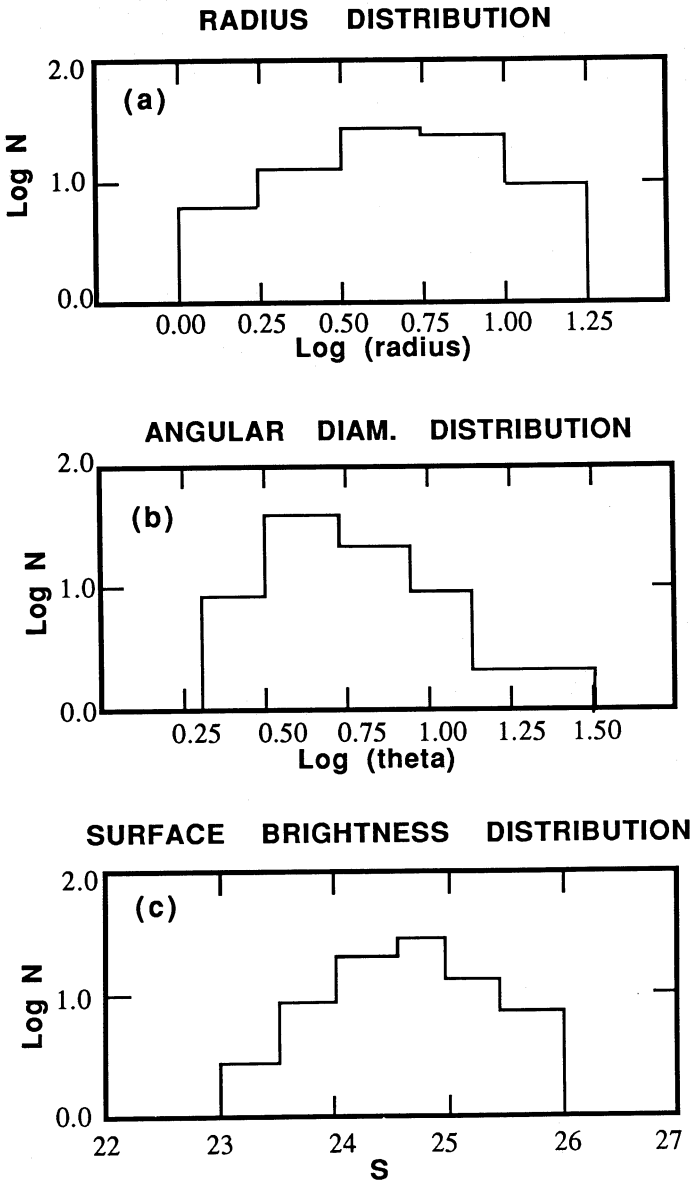

FIG. 2.—Frequency distributions of three properties of the 74 dwarf irregular galaxies brighter than $B_T^0 = 14$. (*a*) Radius distribution (kpc), (*b*) angular diameter distribution (arcmin), (*c*) surface brightness distribution (mag arcsec^{-2}). Notice that all three distributions turn over (especially the radius and surface brightness distributions) well before the lower/dimmer limit is reached.

distributed randomly in space out to the distance (25 Mpc) beyond which the most luminous galaxy falls below the limiting apparent magnitude of the real data. The galaxies were sampled as a stochastic process at a random time yielding luminosity, surface brightness, angular diameter, apparent magnitude, and "optical" radius. In a self-propagating star formation model with intermittent bursts we do not expect the entire surface of the galaxy to be visible—especially for the smallest of galaxies. The "optical" radius is therefore taken to be somewhat smaller than the radius of the H I threshold for star formation. We infer from the galaxy's burst history that the correction takes the form $r_{\rm opt} = r_{\rm H\,I}$ for $r > 2$ kpc, and $r_{\rm opt} = 0.7(r_{\rm H\,I})^{1.5}$ for $r_{\rm H\,I} \leq 2$ kpc.

Objects whose apparent magnitude, surface brightness, or angular diameter fell outside the limits displayed by the real data were then weeded out, leaving a selection of simulated galaxies which could be used for statistical comparison.

IV. ESTIMATE OF GAMMA

Comparison of the simulated and real catalog indicates that the best agreement occurs for a value of the exponent in the adopted power-law radius distribution of $\gamma = -4.2 \pm 0.2$. This conclusion is based on the following considerations:

1. A visual comparison of the frequency distributions of M_B and radius, shown in Figures 3*a* and 3*b*, suggests that γ must be close to -4. (The distribution of angular diameters turns out not to be very sensitive to γ. For any negative γ the nearby detectable galaxies are mostly small, and the distant detectable galaxies are mostly large. Any strong variations in angular size for different γ's is very much reduced by this selection effect.)
2. The mean values, $\langle r \rangle$ and $\langle M_B \rangle$, of the real data each yield nearly identical γ's when compared with the simulations, as shown in Figure 4, and these values bracket $\gamma = -4.2$.
3. An application of the Kolmogorov-Smirnov (K-S) test for the M_B and radius distributions tested the hypothesis that the simulated and real samples were drawn from the same population. The maximum difference between the normalized cumulative distribution of the simulated and real samples was compared with K-S statistic tables given by Miller (1956) and Gibbons (1976, p. 388). The results, displayed in Figure 5, indicated that all of the values of γ except -4.2 ± 0.2 may be rejected at the 95% confidence level or higher.

We therefore conclude that the true frequency distribution of radii for dwarf irregular galaxies is

$$f(r) = Kr^{-4.2} . \quad (1)$$

This result is independent of the adopted distance scale because all the relevant self-propagating star formation parameters scale with H_0. The models of GSS are scale independent. The salient features that describe the episodic burst behavior of dwarf galaxies are related to the adopted star forming "cell" size and galaxy size in units of these cells. Small values of H_0 admit farther galaxies, larger masses, and higher luminosities. The modeling would, of course, take this into account thus rendering an observationally identical simulation. The normalization constant for the selection of 74 galaxies was determined to be $K = 3$ (for r in kpc and density in Mpc^{-3}). The adopted lower limit of galaxy sizes $r_{\rm min}$ is unknown, but does not affect the derived γ, only the derived galaxy number density. For example, the predicted total space density of dwarf irregulars is 160 Mpc^{-3} if $r_{\rm min} \approx 200$ pc, but is 10 Mpc^{-3} if $r_{\rm min} \approx 500$ pc. As shown in Tyson (1988), an attempt to constrain this lower limit found that matching the Lyα high column density absorbers in QSO spectra provides $r_L \sim 500$ pc, so we suggest that the mean dwarf galaxy density is at least 10 Mpc^{-3}.

The model parametrizations that were established from the self-propagating star formation history of dwarf galaxies are considered to be somewhat uncertain. We may then ask if the chosen value of γ is sensitive to the details of the adopted relations. Figure 6 shows the mean absolute magnitude, $\langle M \rangle$, versus mean radius, $\langle r \rangle$, for $\gamma = -2, -3, -4, -5$ and the following five altered star formation scenarios: (1) *cross*, original simulation as described earlier in the text (shown with curve); (2) *diamond*; δ-function burst amplitude distribution; (3) *box*; flat distribution of amplitudes; (4) *circle*; δ-function

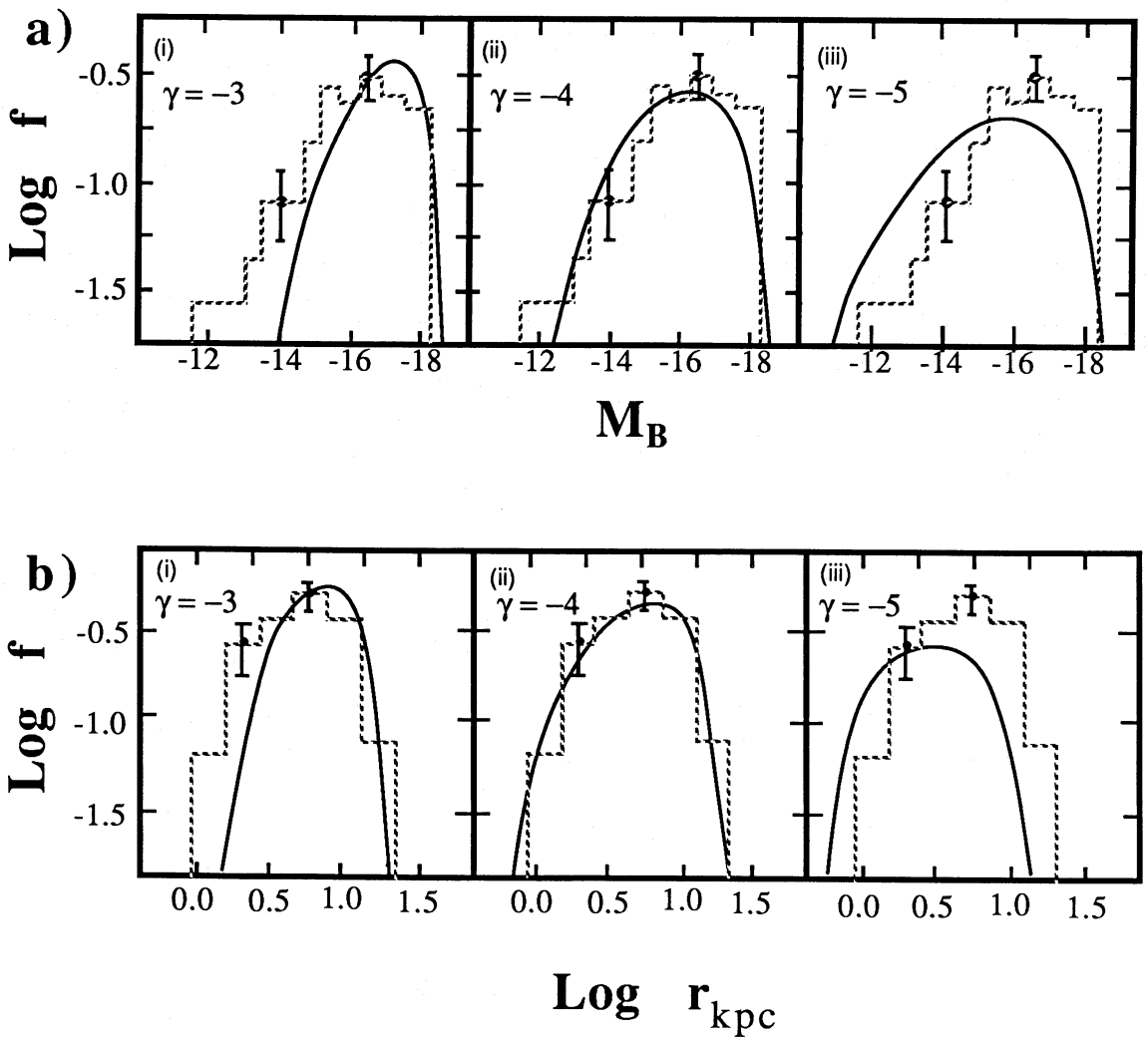

FIG. 3.—Frequency distributions of M_B (*a*) and radius (*b*) for the real data (*histogram*) are plotted along with the simulations (*smooth curve*) for radius frequency distribution exponents (i) $\gamma = -3$, (ii) $\gamma = -4$, (iii) $\gamma = -5$. Note that, visually, $\gamma = -4$ provides the best fit to the histograms.

distribution of burst periods; (5) *asterisk*; flat distribution of burst periods.

Notice from Figure 6 that the variations are clustered for each γ. In fact, for $\gamma = -4.2$, three of the five variations occur within the error bars for the real data. From this information, we can conclude that our resulting γ appears to be more a function of the radius-dependent burst properties (the hallmark of self-propagating star formation) rather than the details of the bursts themselves.

The fact that there was agreement at all for a one-parameter fit to the observations may be interpreted as support for the self-propagating star formation models of GSS.

V. LUMINOSITY FUNCTION

a) Field Galaxies

The observed luminosity function for dwarf irregular galaxies is uncertain, but has been claimed to turn over and decline for $M_B \geq -14$ in a 10 Mpc sample of field galaxies (Kraan-Korteweg and Tammann 1979; Tammann and Kraan-Korteweg 1978) and in the Virgo cluster (Binggeli, Sandage, and Tammann 1985). Our simulations indicate that this may be an artifact of selection effects associated with limiting surface brightness and angular diameter. (We look more closely at the Virgo cluster in § V*b*.) Figure 7*a* shows the frequency distribution of absolute magnitude for the $\gamma = -4.2$ simulation with (A) no selection effects, (B) only the surface brightness limit imposed, (C) only the angular diameter limit imposed, and (D) both the surface brightness and angular diameter limits imposed. (The cutoff at $M_B = -7$ for distribution A is a computing convenience which has no effect on distribution D.) The observed turnover at $M_B \approx -14$ may therefore be attributed to selection effects. The value of M_B at the apparent turnover is not sensitive to the value of γ adopted in the simulations. As we will show below, it is primarily related to the approximate magnitude where galaxies begin to fall below the surface brightness turnover.

Another way to look at the severity of the selection effects may be found in Figure 8. Here we plot absolute magnitude versus log radius for all galaxies "detected" in the simulations (*crosses*), and we plot a small subset of the thousands of galaxies *not* detected in the simulations (*circles*). The solid diagonal lines are lines of constant surface brightness, and the the dotted diagonal line is the surface brightness of the night sky in

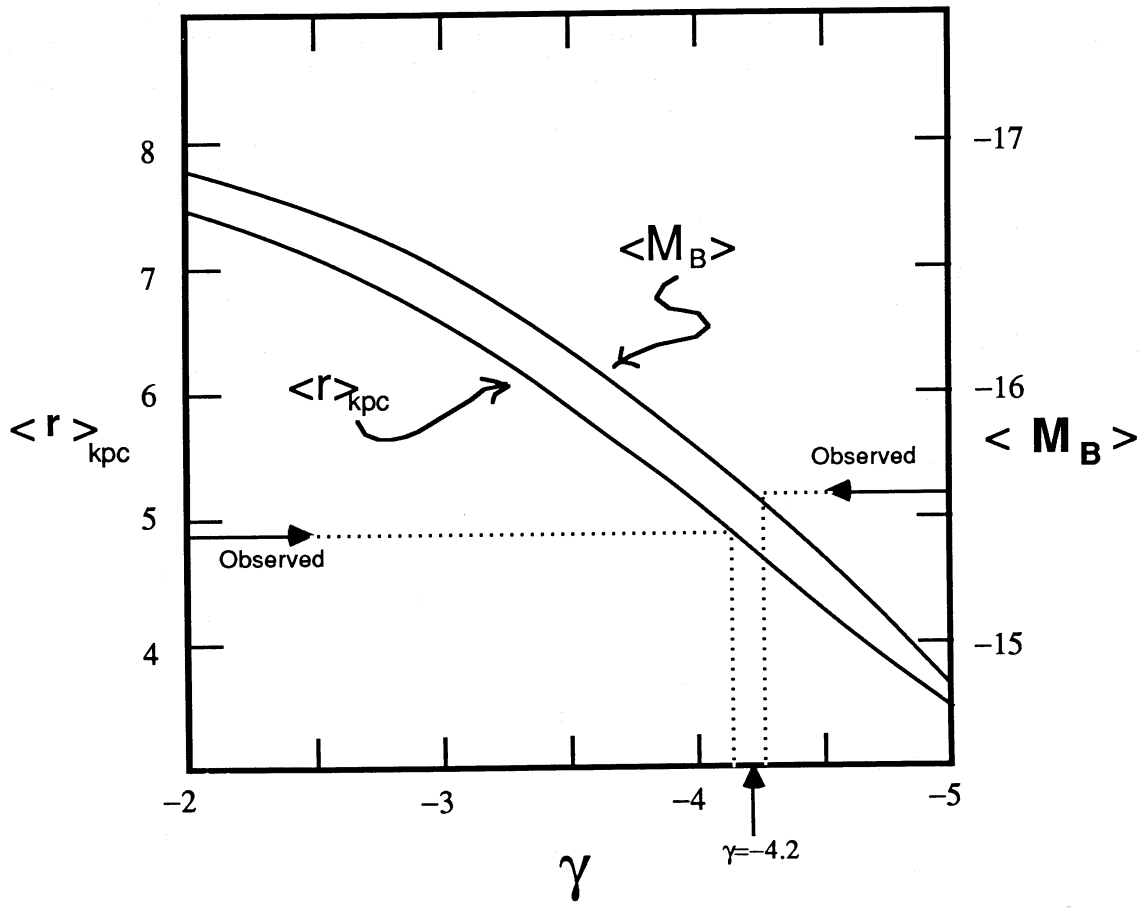

FIG. 4.—Test for the best fit γ is shown. The mean values $\langle r \rangle$ and $\langle M_B \rangle$ of the simulations are shown as a function of γ. Two curves intersect the observed values only for $\gamma = -4.2 \pm 0.2$.

the B band. The galaxies cross the $S = 25$ mag arcsec^{-2} line at about $M_B = -14 \pm 1$. Since Figure 2*c* shows that the surface brightness distribution turns over at about $S = 25$ mag arcsec^{-2} (as is true with the simulation), we have located the primary source of the turnover point in the observed luminosity function.

We find these selection effects to be most severe for bursting galaxies in the SSPSF scenario. When a galaxy spends some of its time "on" and most of its time "off," no inferences can be made about missing dwarfs in a sample without also modeling their star formation history. The severity of this problem does not apply to dwarf ellipticals because trends in the properties of those that are observed may be extended below the detection limits with much greater confidence because they are unlikely to be bursting. In addition, we expect the size-luminosity relationship to be much better behaved for dwarf ellipticals than for bursting dwarfs. An observed catalog is therefore more likely to be complete to a given size for dwarf ellipticals than for dwarf irregulars.

We conclude that the observed luminosity function of bursting galaxies in the SSPSF model is consistent with a luminosity function which continues to increase with decreasing luminosity for $M_B \geq -14$.

b) Cluster Galaxies

Our study was repeated for the "amorphous," "Im," and "BCD" galaxies that are definite members of the Virgo cluster as published in the Virgo Cluster catalog (Binggeli, Sandage, and Tammann 1985, hereafter BST; Sandage, Binggeli, and Tammann 1985, hereafter SBT; Sandage and Binggeli 1984). These galaxies display a roughly Gaussian luminosity function with a broad peak (as does the Kraan-Korteweg and Tammann 1979 sample). We now attempt to show, as we did for the field galaxies, that the observed turnover is an artifact caused by selection effects, and that the true luminosity function continues to increase down to the faintest galaxies.

There were 93 galaxies that were brighter than the catalog completeness limit of $B_T = 18$. Their apparent magnitude limit is not, however, appropriate for comparison with our simulations of dwarf galaxies. We suggest that this limit, which applies to their entire catalog of 2096 galaxies, does *not* simultaneously apply to the morphological subset of amorphous, Im and BCD galaxies. The luminosity distribution of these galaxies begins to turn over at $B_T \approx 15.25$—we take this as the limiting magnitude of our simulation.

Only 28 galaxies were brighter than this detection limit which obviously precludes us from conducting a rigorous statistical comparison. We therefore only looked for gross differences as a secondary check of our radius distribution.

The detection limits, based on the 28 remaining galaxies brighter than $B_T = 15.25$ are angular diameter $\theta > 30''$ (corresponding to $r_{25.5} > 1$ kpc) and mean surface brightness $m'_B < 25$ mag arcsec^{-2}. For our simulations we converted from $r_{26.5}$ to $r_{25.5}$ by assuming an exponential disk, $I(r) = I_0 e^{-\alpha r}$,

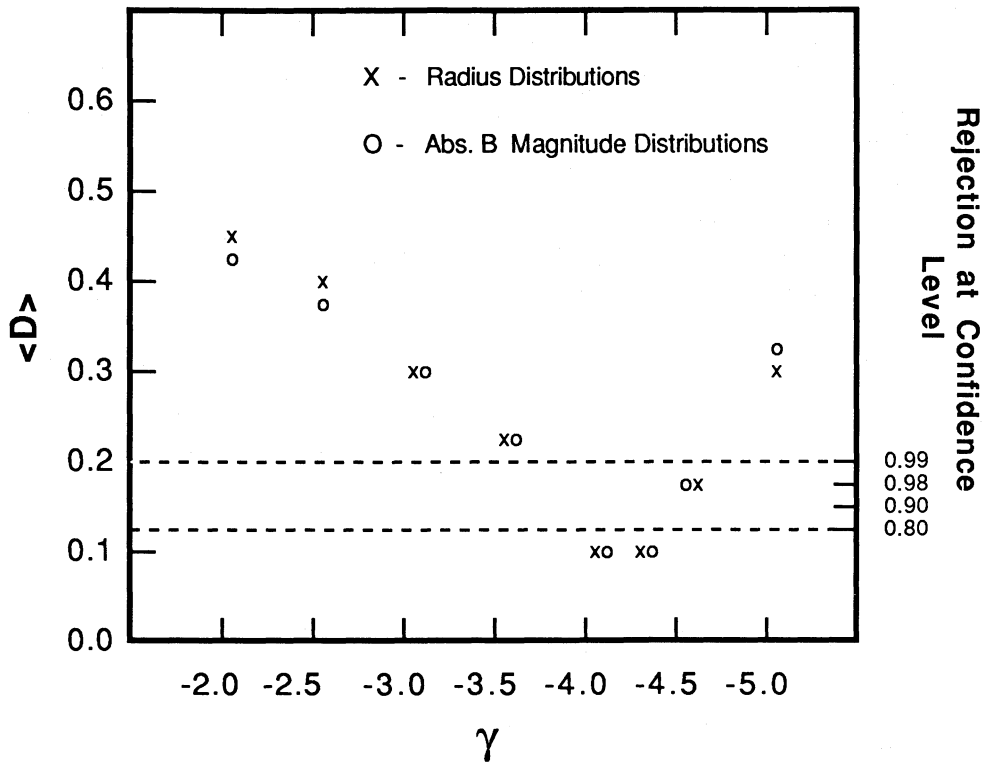

FIG. 5.—Nonparametric Kolmogorov-Smirnov statistical test to determine if the simulations and the real data set were drawn from the same population. The normalized mean difference, $\langle D \rangle$, is plotted against γ. Note the strong dependence of $\langle D \rangle$ on γ. All γ may be rejected at a 95% confidence level or better except for $\gamma = -4.2 \pm 0.2$.

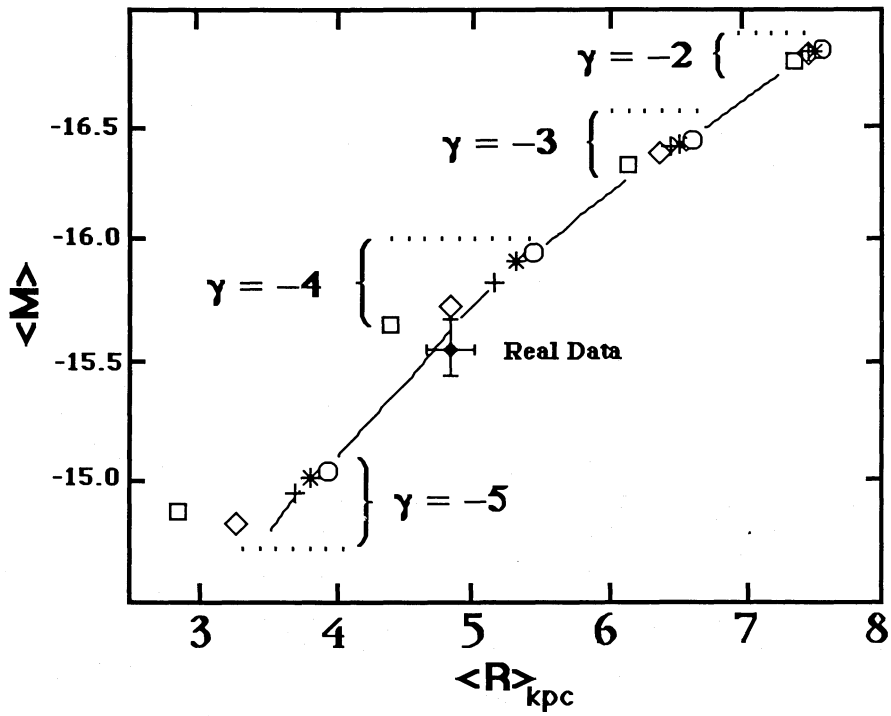

FIG. 6.—Mean absolute magnitude is plotted against the mean radius for four different γ's and five altered star formation scenarios. Crosses show the original simulation. Diamonds refer to a burst history in which all amplitudes are identical (and set equal to the average of the original simulation). Squares refer to a burst amplitude distribution that is uniformly distributed between small and large bursts. Circles represent a constant time difference (equal to the mean of the original simulation) between successive bursts. Asterisks refer to burst separations that are uniformly distributed between short and long periods.

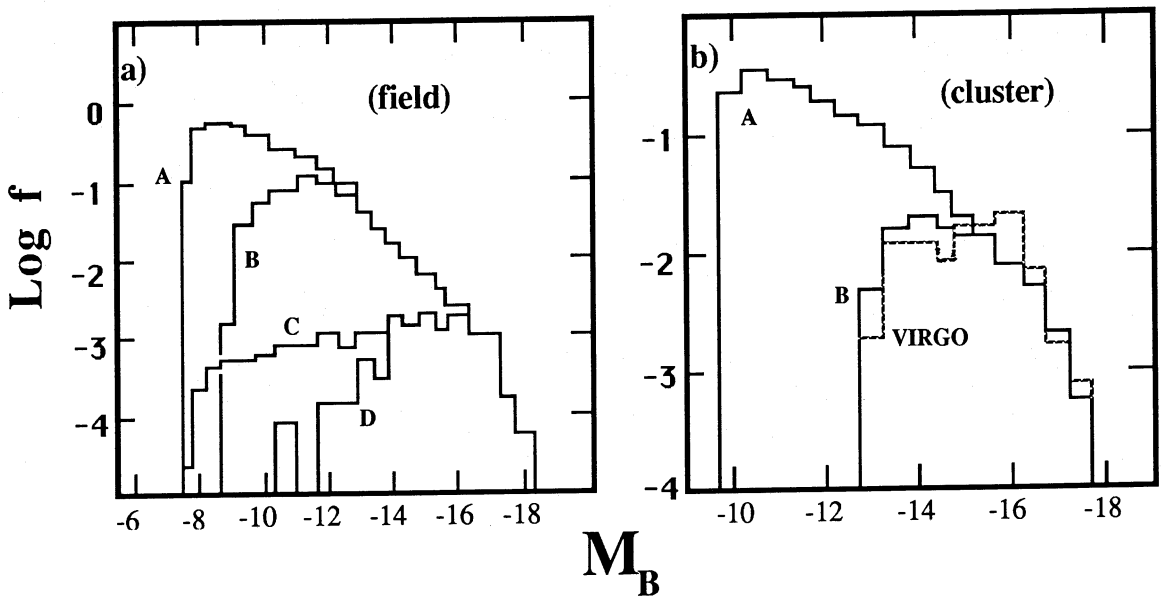

FIG. 7.—(*a*) The simulated luminosity function for field dwarf galaxies showing the results of various selection effects: (A) no selection effects; (B) only the surface brightness limit imposed; (C) only the angular diameter limit imposed; (D) both surface brightness and angular diameter limit imposed. Note the resultant broad "turnover" in the luminosity function D from $M_B = -16$ to -14. The cutoff at $M_B \approx -7$ for distribution A is a computing convenience which has no effect on distribution D. (*b*) Simulated luminosity function for cluster dwarf irregular galaxies. Dashed histogram shows the Sandage, Binggeli, and Tammann (1985) luninosity function for star-forming dwarf galaxies in the Virgo cluster (scaled to our sample size). It is plotted with two luminosity functions from the simulated dwarf galaxies. Histogram A is the luminosity function that would be observed if there were no selection effects of any kind. Histogram B resulted from imposing surface brightness and angular size detection criteria obtained from the galaxies brighter than the turnover, and extending the magnitude limit to $B_T = 18$. Notice the agreement between histogram B and the dashed histogram of the Virgo star-forming dwarfs.

with a scale length $\alpha^{-1} = 1$ kpc (Gallagher and Hunter 1984). Strictly speaking, an exponential disk only exists in the "equivalent profile" of these dwarfs (see, e.g., Mould *et al.* 1986; de Vaucouleurs and Freeman 1972), so we must consider the conversions as approximate. From these steps the computed size of the galaxies was reduced by an average of 30%.

The simulations (using an assumed distance of 16 Mpc for all galaxies) showed that the same value of the exponent in the radius distribution function, $\gamma = -4.2$, produced the best fit to the mean absolute magnitude of the Virgo sample ($\langle M_B \rangle_{\rm sim} = -16.4$, $\langle M_B \rangle_{\rm vir} = -16.3 \pm 0.1$) and the mean radius ($\langle r \rangle_{\rm sim} = 3.9$ kpc, $\langle r \rangle_{\rm vir} = 3.6 \pm 0.3$ kpc). These results lend added confidence to our derived value of γ, and may again be taken as support for the SSPSF model or one with similar properties.

We now continue with our contention that the turnover in the observed luminosity function is an artifact. When we lowered the detection limit of the simulation to $B_T = 18$ (the completeness limit of the entire Virgo catalog) a simulated luminosity function was generated that was indistinguishable from the amorphous + Im + BCD luminosity function of SBT. The dotted histogram in Figure 7*b* shows SBT's luminosity function (scaled to our sample size) plotted with two luminosity functions for the simulated dwarf gaalxies. Histogram A is the luminosity function that one would observe if there were no selection effects of any kind. Histogram B resulted from setting the limiting magnitude to $B_T = 18$ while keeping the surface brightness and angular size limits that were indicated by the 28 dwarf irregular galaxies brighter than $B_T = 15.25$.

We therefore confirm for the Virgo cluster our general conclusion drawn from field galaxies; the present simulations of intermittently bursting dwarf galaxies indicate that the "turnover" found by SBT in the luminosity function of amorphous + Im + BCD galaxies can be explained as an artifact of selection effects that are not properly recognized when the apparent magnitude completeness limit of the entire catalog is assumed to coincide with that of star-forming dwarf galaxies.

VI. DWARF GALAXIES AND THE COSMOLOGICAL DENSITY

In order to predict the contribution of unseen dwarf galaxies to the cosmological density parameter Ω, a relation between mass and radius is required. Masses of galaxies are notoriously difficult to determine accurately for large, "normal" galaxies (see Faber and Gallagher 1979 for review) and are even more difficult to determine for dwarf irregular galaxies; inclinations are uncertain, and velocities may be turbulent rather than gravitational in origin (Allsopp 1978; Sargent *et al.* 1983; Sargent and Lo 1985).

Fisher and Tully (1975) and Thuan and Seitzer (1979) give H I masses for all dwarfs detected in their surveys. They also give total "indicated" masses inferred from H I line widths for those detections with inclination angles greater than 30°. There were 42 galaxies out of the 74 that had "indicated" masses. To improve our statistics we approximated the total mass of the remaining 32 galaxies by assuming that the total mass of gas (including He and molecules) is $M_{\rm gas} = 1.34 M_{\rm H\,I}$, and that the total mass is $M_T = 4 M_{\rm gas}$ based on the value $\langle M_{\rm gas}/M_T \rangle = 0.23 + 0.2/-0.1$ for the 42 galaxies with "indicated" masses. Figure 9 plots the log of the total mass versus log $r_{26.5}$ for all 74 dwarfs. A least-squares fit was generated, but as expected, there is much scatter around the relation:

$$M(r) = K_M r^a , \qquad (2)$$

where $\log K_M = 8.06 \pm 0.15$ and $a = 1.82 \pm 0.25$. The

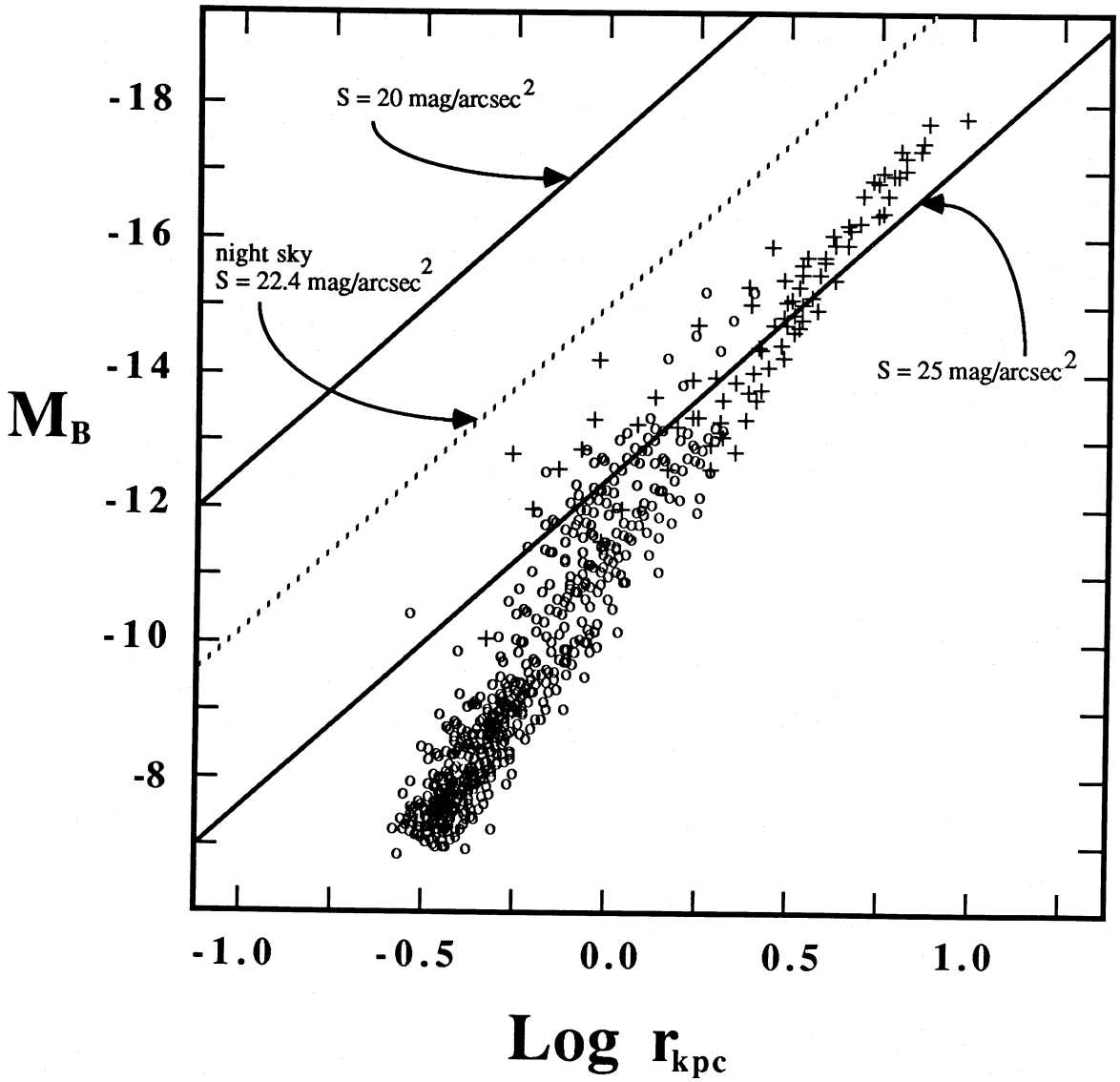

FIG. 8.—Absolute B magnitude for dwarf galaxies is plotted with their log radius in kpc. Diagonal lines are lines of constant surface brightness, of which the dotted line is the surface brightness of the night sky in the B band. Circles represent a small subset of the thousands of undetected galaxies in the sample volume. (Compare with histogram A of Fig. 7*a*.) Crosses represent galaxies "detected" in the computer simulations. (Compare with histogram D of Fig. 7*a*.)

logarithmic slope, $a = 1.8$, is consistent with the estimates of Matteucci and Chiosi (1983) and is somewhat less than what was found by Hoffman *et al.* (1985). Note, however, that Hoffman *et al.* (1985) included Sc–Sdm galaxies in their relation.

The 74 galaxies used for this study represent an observationally selected sample. In spite of this, we are not given reason to expect the *form* of the mass-radius relation to be sensitive to selection effects.

Using the adopted mass-radius relation and radius distribution (eqs. [1] and [2]) we compute

$$\Omega_{\rm dwarf} = \rho/\rho_{\rm crit} = 1/\rho_{\rm crit} \int M(r) f(r) dr$$

$$= 1/\rho_{\rm crit} K_M K_r \int r^a r^\gamma dr \qquad (3)$$

Using $K_r = 3$ Mpc^{-3}, $K_M = 1.15 \times 10^8 M_0$, $\rho_{\rm crit} = 2 \times 10^{-29}$ g cm^{-3}, $a = 1.82$, $\gamma = -4.2$, and knowing that $r_{\rm min}$ is much smaller than $r_{\rm max}$, we get

$$\Omega_{\rm dwarf} \approx 0.0013 (r_{\rm min}/{\rm kpc})^{-1.38} (H_0 = 100 \text{ km s}^{-1} \text{ Mpc}^{-1}) . \qquad (4)$$

Figure 10 shows $\Omega_{\rm dwarf}$ as a function of $r_{\rm min}$. The $\Omega_{\rm dwarf}$ range that is admissible within the 1 σ error bars of the mass-radius relation is noted by the solid curves.

The masses derived for all galaxies (in Fig. 9, and elsewhere) are only the masses within the visible limits of each galaxy. There is evidence for dark matter in dwarf irregular galaxies as indicated by mass-to-light ratios in the range 10 → 30 (Sargent and Lo 1985), and in some cases, mass-to-light ratios greater than 100 (Lake and Schommer 1984). If these high M/L's prove to be common for dwarfs then the value of $\Omega_{\rm dwarf}$ shown by the present simulations could easily approach unity.

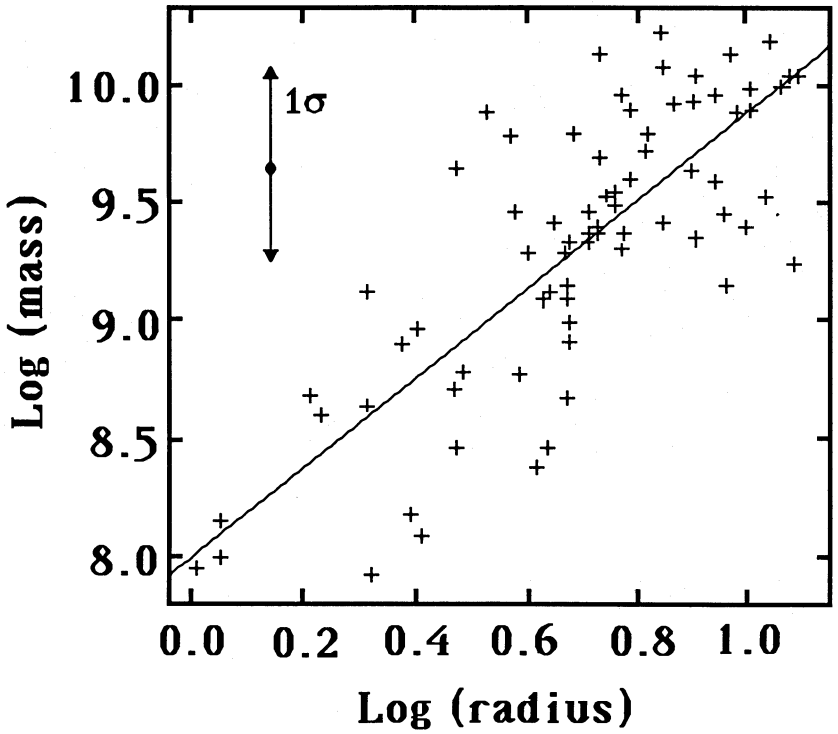

FIG. 9.—The log galaxy mass (solar) vs. the log $r_{26.5}$ for the 74 dwarf irregular galaxies. The fitted relation takes the form: $\log M = 1.82 \log r + 8.06$.

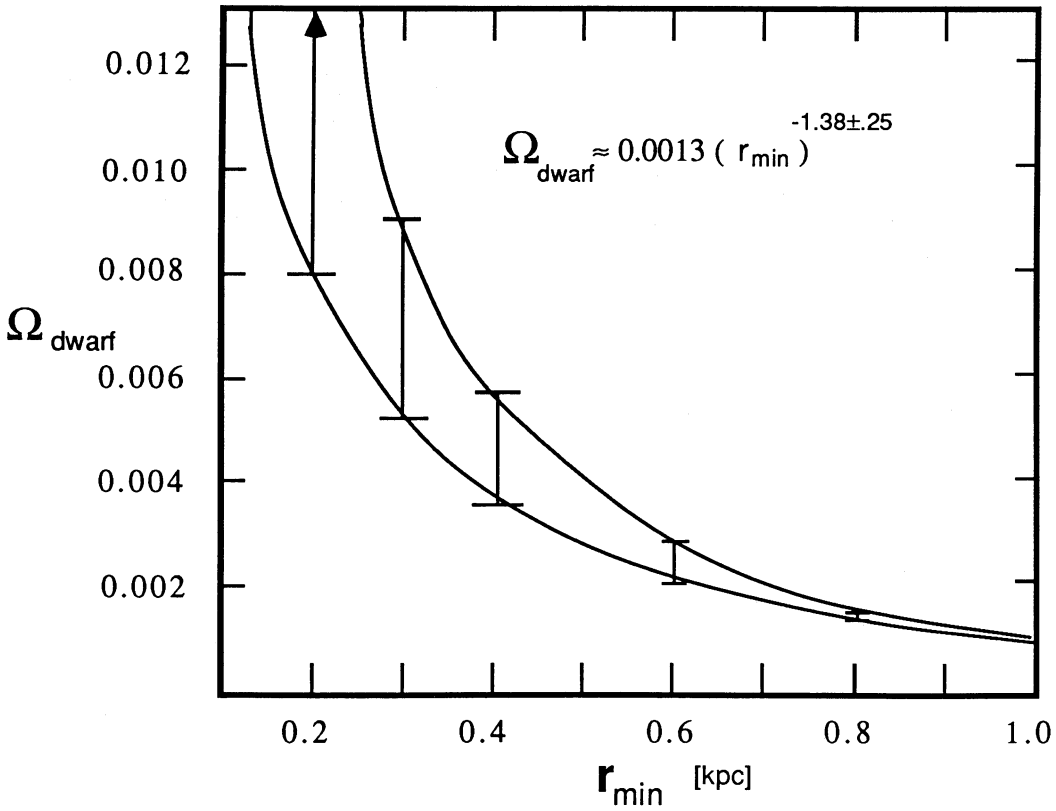

FIG. 10.—Cosmological density parameter is shown to be a sensitive function of the (unknown) lower radius cutoff for dwarf galaxies

VII. DISCUSSION

The number density inferred from the field galaxy simulations is consistent with the upper limits for H I clouds found by Lo and Sargent (1979) using the 40 m Owens Valley radio telescope. When converted to the "short" distance scale for these groups (de Vaucouleurs 1979) the comparison is as follows: M81 group, $n_{\text{Lo-Sarg}} = 0.51$ Mpc^{-3} and $n_{\text{sim}} = 0.43$ Mpc^{-3}; CVnI group, $n_{\text{Lo-Sarg}} = 0.28$ Mpc^{-3} and $n_{\text{sim}} = 0.08$ Mpc^{-3}; N1023 group, $n_{\text{Lo-Sarg}} = 0.07$ Mpc^{-3} and $n_{\text{sim}} = 0.01$ Mpc^{-3}. For this comparison we assumed $M_{\text{H I}} \approx 0.25 M_{\text{tot}}$ (as indicated by this work), and converted the Lo and Sargent (1979) mass detection limits to a galaxy radius via the mass-radius relation of § VI. From the galaxy radius we computed the number density for $\gamma = -4.2$. We note that when Lo and Sargent (1979) used a 100 m telescope on small selected areas within their target groups they detected four previously uncataloged dwarf galaxies. These detections are just the "tip of the iceberg" if our results are correct.

We are currently investigating the uniqueness of the SSPSF results by modeling dwarfs in which star formation is assumed to be induced purely by tidal encounters with neighboring galaxies. We are also estimating the expected detection rate of "intergalactic" supernovae which are associated with invisible dwarf galaxies.

We thank G. de Vaucouleurs, H. Corwin, P. Seiden, J. A. Tyson, and R. Buta for helpful discussions and an anonymous referee for several constructive comments and suggestions. One of us (N. D. T.) wishes to thank the Astronomy Program of the University of Maryland for the release time given to complete this work.

REFERENCES

Allsopp, N. J. 1978, *M.N.R.A.S.*, **184**, 397.
Arp, H. 1965, *Ap. J. (Letters)*, **142**, L401.
Binggeli, B., Sandage, A., and Tammann, G. A. 1985, *A.J.*, **90**, 1681 (BST).
Bothun, G. D., Impey, C., and Mann, B. 1986, *Bull. AAS*, **18**, 958.
Bothun, G. D., Mould, J. R., Caldwell, N., and MacGillivray, H. T. 1986, *A.J.*, **92**, 1007.
Buta, R. 1986, private communication.
———. 1987, *Ap. J. Suppl.*, **64**, 1.
de Vaucouleurs, G. 1975, in *Stars and Stellar Systems, Galaxies and the Universe*, ed. A. Sandage, M. Sandage, and J. Christian (Chicago: University of Chicago Press), p. 557.
———. 1978*a*, *Ap. J.*, **223**, 730.
———. 1978*b*, *Ap. J.*, **224**, 710.
———. 1979, *Ap. J.*, **227**, 729.
de Vaucouleurs, G., de Vaucouleurs, A., and Buta, R. 1981, *A.J.*, **86**, 1429.
———. 1983, *A.J.*, **88**, 764.
de Vaucouleurs, G., and Freeman, K. C. 1972, *Vistas Astr.*, **14**, 163.
Disney, M. J. 1976, *Nature*, **263**, 573.
Faber, S. M., and Gallagher, J. S. 1979, *Ann. Rev. Astr. Ap.*, **17**, 135.
Fisher, J. R., and Tully, R. B. 1975, *Astr. Ap.*, **44**, 151.
Gallagher, J. S., and Hunter, D. A. 1984, *Ann. Rev. Astr. Ap.*, **22**, 37.
Gerola, H., Seiden, P. E., and Schulman, L. S. 1980, *Ap. J.*, **242**, 517 (GSS).
Gibbons, J. D. 1976, *Non-Parametric Methods for Quant. Analysis* (New York: Holt, Rinehart & Winston).
Hoffman, G. L., Helou, G., Salpeter, E. E., and Sandage, A. 1985, *Ap. J. (Letters)*, **289**, L15.
Holmberg, E. 1958, *Medd. Lunds Astr. Obs.* ser. 2, No. 136.
Huchtmeier, W. K., Seiradakis, J. H., and Materne, J. 1981, *Astr. Ap.*, **102**, 134.
Hunter, D. A., and Gallagher, J. S. 1985, *A.J.*, **90**, 1789.
Kraan-Korteweg, R. C., and Tammann, G. A. 1979, *Astr. Nach.* **300**, 181.
Kunth, D., Martin, J. M., Maurogordato, S., and Vigraux, L. 1985, *Star-forming Dwarf Galaxies and Related Objects*, ed. D. Kunth, T. X. Thuan, and J. T. T. Van (Paris: Institut d'Astrophysique), p. 89.
Lake, G., and Schommer, R. A. 1984, *Ap. J. (Letters)*, **279**, L19.
Lo, K-Y., and Sargent, W. L. W. 1979, *Ap. J.*, **227**, 756.
Longo, G., and de Vaucouleurs, A. 1983, *Univ. Texas Monogr.*, No. 3.
———. 1985, *Univ. Texas Monogr.*, No. 3A.
Loose, H.-H., and Thuan, T. X. 1985, in *Star-forming Dwarf Galaxies and Related Objects*, ed. D. Kunth, T. X. Thuan, and J. T. T. Van (Paris: Institut d'Astrophysique), p. 73.
Matteucci, F., and Chiosi, C. 1983, *Astr. Ap.*, **123**, 121.
Miller, L. 1956, *J. Am. Stat. Ass.*, **151**, 111.
Mould, J. R., Schneider, D. P., Harding, P., and Bothun, G. D. 1986, *Pub.A.S.P.*, **98**, 732.
Nilson, P. 1973, *Uppsala Astr. Obs. Ann.* Vol. **6**.
Sandage, A., and Binggeli, B. 1984, *A.J.*, **89**, 919.
Sandage, A., Binggeli, B., and Tammann, G. A. 1985, *A.J.*, **90**, 1759.
Sargent, W. L. W., and Lo, K.-Y. 1985, in *Star-forming Dwarf Galaxies and Related Objects*, ed. D. Kunth, T. X. Thuan, and J. T. T. Van (Paris: Institut d'Astrophysique), p. 253.
Sargent, W. L. W., Sancisi, R., and Lo, K-Y. 1983, *Ap. J.*, **265**, 711.
Seiden, P. E. 1983, *Ap. J.*, **266**, 555.
———. 1986, private communication.
Skillman, E. D., and Bothun, G. D. 1986, *Astr. Ap.*, **165**, 45.
Skillman, E. D., Terlevich, R., and van Woerden, H. 1985, in *Star-forming Dwarf Galaxies and Related Objects*, ed. D. Kunth, T. X. Thuan, and J. T. T. Van (Paris: Institut d'Astrophysique), p. 265.
Tammann, G. A., and Kraan-Korteweg, R. C. 1978, in *IAU Symposium 79, The Large Scale Structure of the Universe*, ed. M. S. Longair and J. Einasto (Dordrecht: Reidel), p. 71.
Thuan, T. X., and Seitzer, P. O. 1979, *Ap. J.*, **231**, 327.
Tyson, N. D. 1988, *Ap. J. (Letters)*, in press.
Tyson, J. A., and Jarvis, J. F. 1979, *Ap. J. (Letters)*, **230**, L153.
van den Bergh, S. 1959, *Pub. David Dunlop Obs.*, **2**, 147.

JOHN M. SCALO: Department of Astronomy, University of Texas, Austin, TX 78712

NEIL D. TYSON: Astronomy Program, University of Maryland, College Park, MD 20742